Irregular Scattering of Acoustic Rays by Vortices

V. Pagneux[1] and A. Maurel[2]

[1]*Laboratoire d'Acoustique de l'Université du Maine, UMR CNRS 6613, Avenue Olivier Messiaen, 72085 Le Mans Cedex 9, France*

[2]*Laboratoire Ondes et Acoustique, UMR CNRS 7587, Ecole Supérieure de Physique et de Chimie Industrielles, 10 rue Vauquelin, 75005 Paris, France*

(Received 17 August 2000)

The scattering of high-frequency sound wave, under geometrical acoustic approximation, by three stationary vortices in two dimensions is investigated. For a sufficiently high Mach number of the vortex flow, the scattering of sound rays becomes irregular, displaying a new example of chaotic scattering for a time-reversal breaking system. The fractal dimension, as well as the unstable and stable manifolds of the scattering dynamics, is presented.

DOI: 10.1103/PhysRevLett.86.1199 PACS numbers: 43.20.+g, 05.45.–a, 47.32.–y

Classical scattering, as opposed to wave scattering, is capable of displaying irregular (chaotic) characteristics [1,2]. Such phenomena have already been described for different physical situations (for a review, see [3]). For instance, in classical Hamiltonian mechanics, trajectories of a particle after scattering by three potential hills are very sensitive to initial conditions (i.e., the trajectories before scattering); this is due to the existence of periodic orbits in the region of the three hills. Though the very meaning of the word chaos is not the same for the classical and the quantum case, there are striking consequences of chaos in a classical scattering problem for the corresponding quantum problem [2].

We consider the case of acoustic rays scattered by three vortices. In addition to the interest that this subject has in itself, motivation for this study comes from the development of acoustical techniques, based on the analysis of waves scattered by the medium, to characterize turbulent flows modeled as a set of vortices [4–6]. The aim of this paper is to describe how sound rays are scattered by three vortices; in particular, we show that there exists a critical value of the Mach number $\mathrm{Ma} = U/c$ (where U is the characteristic flow velocity and c is the sound speed) for the appearance of irregular scattering whose dynamical characteristics are analyzed. First, the model equations of sound rays propagating in rotational flow are presented and they are applied in the case of scattering by one vortex. Then, the three-vortex case is investigated and the irregular scattering is studied.

Equations for sound rays propagating in a moving medium can be derived from the wave equation in the limit where the frequency of the sound wave is large compared to the maximum of the two typical frequencies f_1 and f_2 of the problem. Frequency $f_1 = U/L$, where L is the vortex size, is the characteristic flow frequency and $f_2 = c/L$ is related to the time of flight through the vortex. Under this high frequency approximation, the following system of equations is obtained [7,8]:

$$\frac{d\vec{r}}{dt} = c\,\frac{\vec{k}}{k} + \vec{U}\,, \tag{1a}$$

$$\frac{d\vec{k}}{dt} = -(\vec{k}\cdot\vec{\nabla})\vec{U} - \vec{k}\wedge\vec{\mathrm{rot}}\vec{U}\,, \tag{1b}$$

where $\vec{r}$ and $\vec{k}$ are, respectively, the coordinate and the wave vector of the sound wave, and where $\vec{U}$ is the stationary mean flow velocity. In two dimensions, the phase space for the dynamical system (1a) and (1b) has four coordinates x, y, k_x, k_y. The dynamics takes place in a three dimensional subspace since there exists an integral of the motion: Eqs. (1a) and (1b) can be written as an autonomous Hamiltonian system $d\vec{r}/dt = \partial\omega/\partial\vec{k}$ and $d\vec{k}/dt = -\partial\omega/\partial\vec{r}$, and the pulsation $\omega = ck + \vec{U}\cdot\vec{k}$ is an integral of the system. We choose the three remaining coordinates to be x, y, ϕ, where $\phi = (\widehat{\vec{e}_x, \vec{k}})$ is the angular deflection for $\vec{k}$ in the outgoing region (see Fig. 1).

The mean flow is a viscous core vortex with only an orthoradial velocity component:

$$\vec{U} = \frac{\Gamma}{2\pi r}\,[1 - \exp(-\alpha^2 r^2)]\vec{e}_\theta\,.$$

This vortex is characterized by its typical size $r_0 = 1.12/\alpha$ corresponding to the maximum velocity $U_m = 0.716\Gamma/(2\pi r_0)$.

The system [Eqs. (1a) and (1b)] is first numerically integrated for a one vortex case. We use a fourth-order

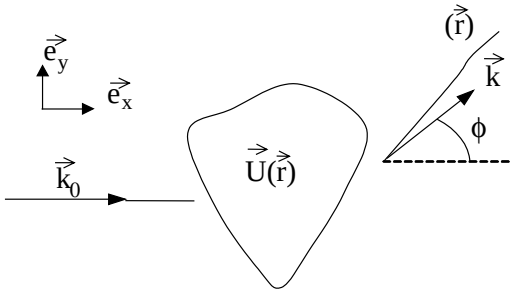

FIG. 1. The scattering process, occurring in the region with $\vec{U}$ flow field, transforms the incoming trajectory into an outgoing one; ϕ is defined as the angular deflection between the two trajectories.

 © 2001 The American Physical Society

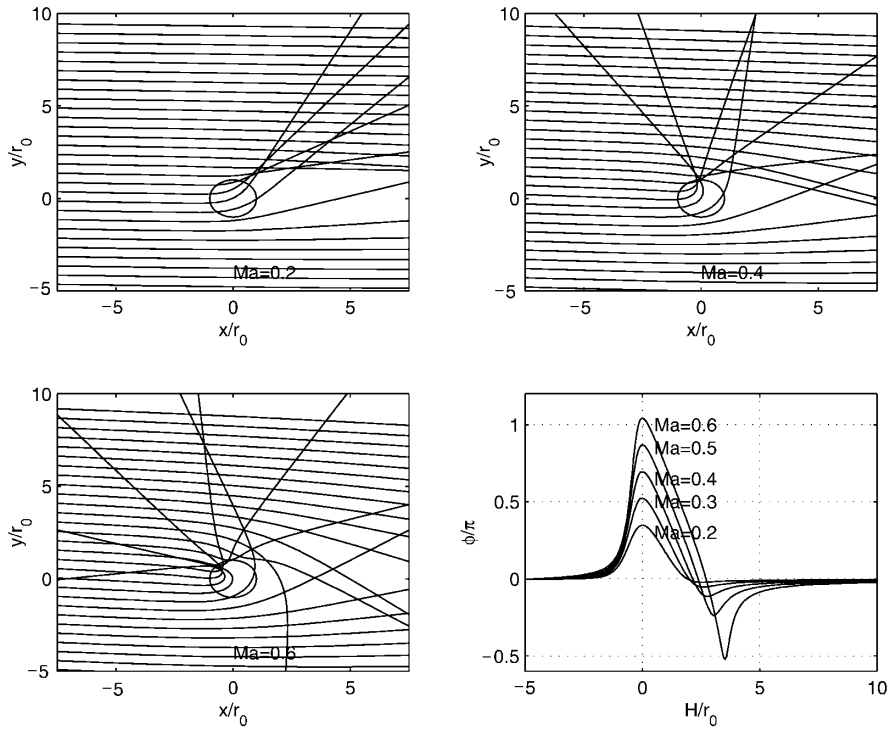

FIG. 2. Ray trajectories in a scattering region with one vortex (the incoming trajectory is defined by $[\vec{r}_0 = (-12r_0, H), \vec{k}_0 = (1,0)]$ for Ma $= 0.2$, 0.4, and 0.5 and scattering function ϕ as a function of H.

Runge-Kutta scheme with adaptative step size. Initial conditions for $\vec{r}$ and $\vec{k}$ are $\vec{r} = (x_0 = -12r_0, y_0 = H)$ and $\vec{k} = (1,0)$. Figure 2 shows the ray trajectories for three different Mach numbers and the scattering function, defined as the angular deflection $\phi(H) = \arctan(k_y/k_x)_{(t=\infty)}$. It has been verified that our results are identical to those already shown in the same case in [9]. When the Mach number varies, the scattering function $\phi(H)$ shows a structural stability in contrast to the case of a particle in a potential hill of height V_0, where there exists a critical value of the kinetic energy $E_c = V_0$; below V_0, $\phi(H = 0) = \pi$ and above V_0, $\phi(H = 0) = 0$. On the other hand, the scattering function is not symmetric with respect to the $y = 0$ line, also in contrast with the case of the potential hill. This is related to the time-reversal violation, observed for the scattering of sound wave by a vortex [10].

What happens now if there are three vortices instead of one? The numerical setup is the following: each vortex is on the apex of an equilateral triangle of side length $5r_0$, as shown in Fig. 3. As before, the initial conditions are $\vec{r} = (x_0 = -12r_0, y_0 = H)$ and $\vec{k} = (1,0)$. The scattering functions for three vortices are shown in Fig. 4. For low Mach numbers, the scattering function $\phi(H)$ is a smoothly varying curve with three bell shape peaks (BSP) centered on the y value of each vortex. As the Mach number is increased, the scattering function behaves wildly in certain regions on the first BSP and this wild behavior persists on an arbitrarily small scale, as illustrated in Fig. 5 at Ma $= 0.6$. This corresponds to chaotic scattering when the impact parameter leads to trajectories near periodic orbits. Indeed, for Ma $= 0.6$, reflection from vortex 2 to vortex 3 at angles up to $2\pi/3$ is possible, as can be seen in Fig. 2. Since most of the usual symmetries are lost, only the first BSP presents this behavior; an impact on the second and third vortex may lead to periodic orbits (and thus to irregular scattering), but for a higher Mach number.

It is then possible to determine the structure of the region where the singularities occur. A singularity is defined by an H value where the scattering function ϕ is not continuous. For the numerical determination of singular points we use the following criterion (inspired by [3]): $[\phi(H + \epsilon) - \phi(H)][\phi(H - \epsilon) - \phi(H)] > 0$, where

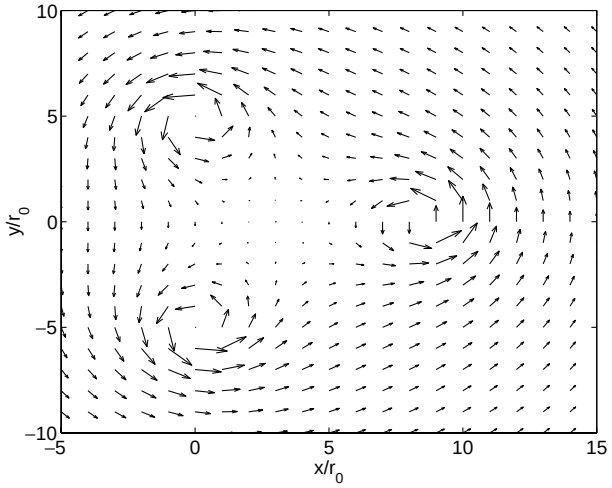

FIG. 3. Scattering region defined by the velocity field $\vec{U}$ induced by three vortices. Vortex 1 corresponds to $y < 0$, vortex 2 to centerline, and vortex 3 to $y > 0$.

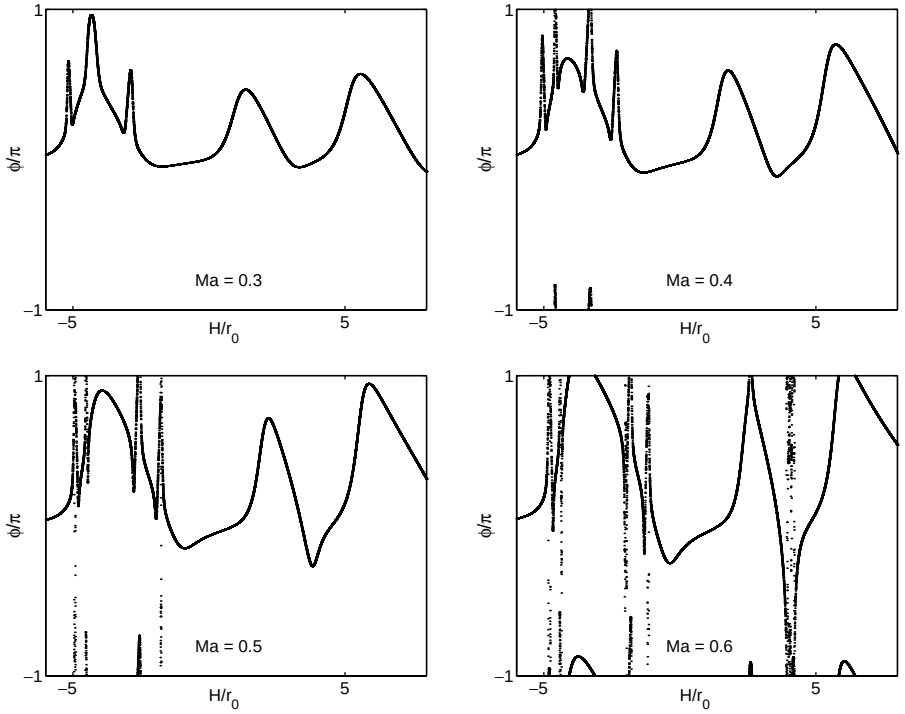

FIG. 4. Scattering function $\phi(H)$ for the three-vortex case at Ma = 0.3, 0.4, 0.5, and 0.6.

the values of H are chosen randomly in an interval containing the region where the irregular scattering occurs. When the criterion is verified, point H is said to be ϵ uncertain. Figure 6(a) shows the evolution of the ϵ uncertain H values for decreasing ϵ; of course, as ϵ goes to zero, fewer and fewer values of H remain ϵ uncertain: these H values correspond to the very sensitive regions where the scattering is irregular (these regions constitute a Cantor set). The fractal dimension of the Cantor set is then determined classically [3]. We call N_t the number of H values tested and N the number of H values found as ϵ uncertain (N depends on ϵ). With $f(\epsilon)$ the limit of N/N_t as N_t goes to infinity [see Fig. 6(b)], $f(\epsilon)$ is expected to scale as ϵ^α, where α is related to the dimension D of the set by the relation $D = 1 - \alpha$. Figure 6 shows the evolution of the fractal dimension as a function of the Mach number. We have determined the shape of the $y = 0$ cross section of the stable and unstable manifolds of the chaotic set (Fig. 7). This has been done by taking a grid of initial conditions (x, θ), with $\theta = (\widehat{\vec{e}_x, \vec{k}})$, and integrating them forward (respectively, backwards) in time.

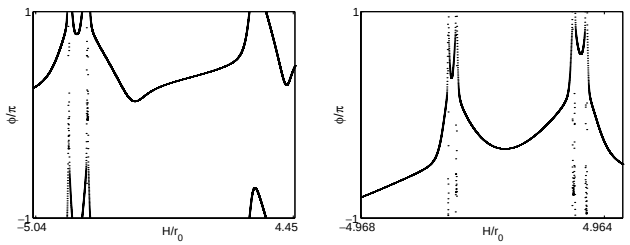

FIG. 5. Scattering function behavior for two successive zooms in Fig. 4 for Ma = 0.6.

We have plotted the time delay (long delays correspond to black regions). Again, the breaking of time-reversal symmetry can be observed. Consider the scatterer positions studied by Jung and Richter [11] for classical potential scattering system $V(x, y) = \exp[-y^2 - (x + \sqrt{2})^2] + \exp[-(y - \sqrt{3/2})^2 - (x - \sqrt{2})^2] + \exp[-(y + \sqrt{3/2})^2 - (x - \sqrt{2})^2]$. The Hamiltonian equation $d\vec{r}/dt = \partial H/\partial \vec{p}$ and $d\vec{p}/dt = -\partial H/\partial \vec{r}$ [with $H(\vec{r}, \vec{p}) = V(\vec{r}) + p^2/2m$] possesses two symmetries: (i) σ defined by σ: $(x, y, p_x, p_y) \rightarrow (x, -y, p_x, -p_y)$ with $t \rightarrow t$ and (ii) time-reversal symmetry T: $(\vec{r}, \vec{p}) \rightarrow (\vec{r}, -\vec{p})$ with $t \rightarrow -t$. The former symmetry implies that the stable (respectively, unstable)

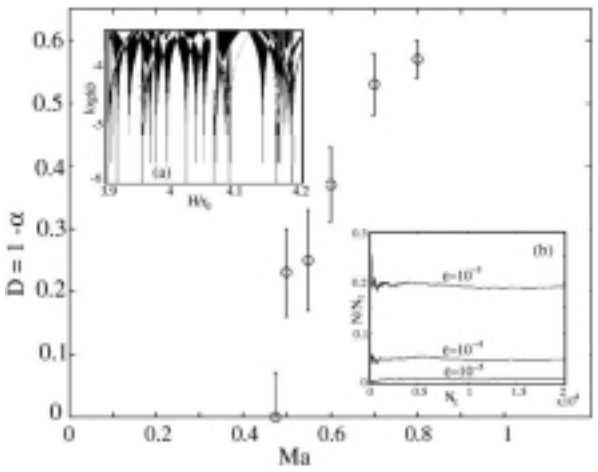

FIG. 6. Fractal dimension as a function of Ma for the three-vortex case. (a) shows the evolution of the ϵ-uncertain values as a function of ϵ and (b) shows the fraction of ϵ-uncertain values as a function of N_t, number of H values tested.

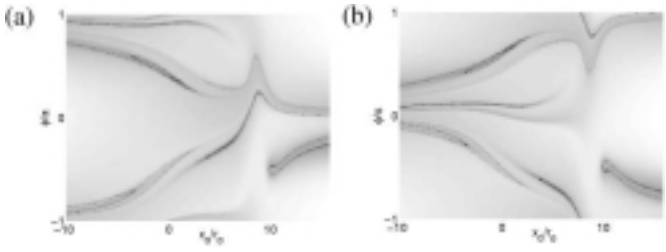

FIG. 7. $y = 0$ cross section of the stable (a) and unstable (b) manifold of the chaotic set.

manifold has the same symmetry as the potential, i.e., in phase space $\theta \rightarrow -\theta$. The latter symmetry implies that the unstable manifold can be deduced from the stable manifold by T, i.e., in the phase space $\theta \rightarrow \pi + \theta$. In our case, the Hamiltonian system, defined by $\omega(\vec{r}, \vec{k}) = ck + \vec{U}(\vec{r}) \cdot \vec{k}$, has lost the symmetries σ and T. To recover the time-reversal invariance, we have to account for the flow velocity field by the transformation $\vec{U}(\vec{r}) \rightarrow -\vec{U}(\vec{r})$ [10]. In our configuration, this transformation is obtained through $To\sigma$. As a consequence, the unstable manifold is deduced from the stable manifold by $To\sigma$, i.e., in phase space $\theta \rightarrow \pi - \theta$. In order to gain insight into the structure of the intersection of the chaotic invariant set with the plane $y = 0$, Fig. 8 shows the product of the delay times shown in Fig. 7 and corresponding to stable and unstable manifolds. Apparently, the intersections between stable and unstable manifolds occur with angles quite different from zero. No tangencies between the stable and unstable manifolds being noticeable, it is reasonable to infer that the dynamics of the scattering is hyperbolic [12,13].

In conclusion, we stress the interest of this new example of chaotic scattering in time-reversal breaking system in classical physics. One may think about experiments intending to complete the present work. One possibility could be to use high Mach number compressible vortices induced by shock-wave diffraction over obstacle or around corners (see, for instance, Mandella's experiments [14],

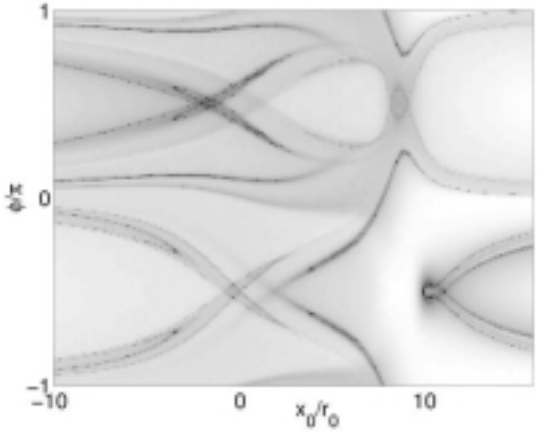

FIG. 8. Intersection of the chaotic invariant set with the plane $y = 0$.

and the confrontation with numerical work [15]). Another possibility could be to use an assembly of vortices: in this case, the critical Mach number for the appearance of chaotic scattering for rays could be significantly decreased and more easily adaptable to classical hydrodynamic setup. Finally, maybe the most promising experimental possibility could be to use the analogy between acoustic and surface water waves. In this latter case, high Mach numbers are easily reachable since the wave celerity is quite low (some dozens of m/s). Note that this analogy has been already extensively used to study the sound wave interaction, both for theory [16–18] and experiments [19].

Two other points seem worthwhile to study in the future, both incidently related to the actual experiment that may be carried out. First, nonstationarity of the vortices could be taken into account and yield nonconstant frequency ω and thus might lead to frequency gap in analogy with the energy gap found for the scattering by two oscillating disks [20]. Second, the very interesting questions raised by the corresponding finite wavelength problem could be partially answered by direct numerical simulation of sound flow equations.

[1] B. Eckart, Physica (Amsterdam) **33D**, 89 (1988).
[2] U. Smilansky, in *Chaos and Quantum Physics*, edited by M.-J. Giannoni, A. Voros, and J. Zinn-Justin (Elsevier, Amsterdam, 1992).
[3] E. Ott, *Chaos in Dynamical Systems* (Cambridge University Press, Cambridge, England, 1993).
[4] C. Baudet, O. Michel, and W. J. Williams, Physica (Amsterdam) **128D**, 1–17 (1999).
[5] R. Labbe and J.-F. Pinton, Phys. Rev. Lett. **81**, 1413 (1998).
[6] D. Boyer and F. Lund, Phys. Rev. E **61**, 1491 (2000).
[7] L. Landau and E. Lifshitz, *Fluid Mechanics* (Pergamon Press, New York, 1959).
[8] T. Colonius, S. K. Lele, and P. Moin, J. Fluid Mech. **260**, 271–298 (1994).
[9] T. M. Georges, J. Acoust. Soc. Am. **51**, 206–209 (1971).
[10] P. Roux and M. Fink, Europhys. Lett. **32**, 25–29 (1995).
[11] C. Jung and P. Richter, J. Phys. A **23**, 2847–2866 (1990).
[12] S. Bleher, E. Ott, and C. Grebogi, Phys. Rev. Lett. **63**, 919 (1989).
[13] S. Bleher, C. Grebogi, and E. Ott, Physica (Amsterdam) **46D**, 87–121 (1990).
[14] M. J. Mandella, Y. J. Moon, and D. Bershader, *Shock Waves and Shock Tubes*, edited by D. Bershader and R. Hanson (Stanford University Press, Stanford, CA, 1986), pp. 471–477.
[15] T. Colonius, S. K. Lele, and P. Moin, J. Fluid Mech. **230**, 45–73 (1991).
[16] E. Cerda and F. Lund, Phys. Rev. Lett. **70**, 3896 (1993).
[17] C. Coste, F. Lund, and M. Umeki, Phys. Rev. E **60**, 4908 (1999).
[18] C. Coste and F. Lund, Phys. Rev. E **60**, 4917 (1999).
[19] F. Vivanco, F. Melo, C. Coste, and F. Lund, Phys. Rev. Lett. **83**, 1966 (1999).
[20] A. Antillón, J. V. José, and T. H. Seligman, Phys. Rev. E **58**, 1780 (1998).